Effect of Configuration of Micro-/Nanoscale Structure on Sliding Surface on Molecular Gas-Film Lubrication

Susumu Isono[*], Masashi Yamaguchi[*], Shigeru Yonemura[*], Takanori Takeno[†], Hiroyuki Miki[*] and Toshiyuki Takagi[*]

[*] *Institute of Fluid Science, Tohoku University, Katahira 2-1-1, Aoba-ku, Sendai 980-8577, Japan*
[†] *Tohoku University International Advanced Research and Education Organization, Aoba 6-3, Aramaki, Aoba-ku, Sendai, 980-8578, Japan*

Abstract. Nakamori *et al*. found experimentally that the friction between a partly polished diamond coating and a metal surface was drastically reduced to zero as relative speed increased to a few m/s [*Diamond Relat. Mater.* 14, (2005), 2122]. It seems that diamond coating took off the counter surface because sliding was noiseless in their experiment. However, the mechanism of this phenomenon was unknown. In the previous work, we performed the numerical simulation of micro-/nanoscale gas flow between two sliding surfaces, i. e., the slider surface with microscale surface roughness like partly polished diamond coating and the flat counter surface. And then, we successfully reproduced lift force large enough to suspend the slider used in the experiment and found that this effect became notable only for micro-/nanoscale gas flow. In the present paper, we investigate the effect of configuration of micro-/nanoscale structure on sliding surface on molecular gas-film lubrication. Since micro-/nanoscale gas flows between two sliding surfaces cannot be treated as a continuum, we use the direct simulation Monte Carlo (DSMC) method.

Keywords: Molecular gas-film lubrication, Diamond coating, Micro-nanoscale flow, DSMC method
PACS: 47.85.mf, 47.61.-k, 46.55.+d, 47.45.-n

INTRODUCTION

Recently, molecular gas-film lubrication (MGL) has aroused the industrial interest. For example, flying head slider in hard drive (HDD) is suspended slightly above a rotating magnetic disk by molecular gas film. In order to realize high memory density, keeping spacing between the flying head and the disk to be small is important. The spacing is about 10 nm in the current HDD. The flying head is lifted by molecular gas flow in the spacing.

On the other hand, diamond coating is well known as low friction material and is expected to apply to sliding surfaces. Nakamori *et al*. [1] found experimentally that the friction between a diamond coating with partly polished surface and a metal surface was drastically reduced to zero as relative speed increased to a few m/s. Their experimental setup and their results are shown in Figs. 1 and 2, respectively. Diamond films were deposited onto TiC substrates by hot filament CVD [2]. This sliding was noiseless during their experiment. This indicates that the slider took off the counter metallic surface, that is, the mechanism of this sliding was not the boundary lubrication, but the gas-film lubrication. However, the floating mechanism was unknown. The goal of our research is to solve the floating mechanism of this phenomenon and to propose the new gas lubrication system by applying this phenomenon.

The mean free path λ of atmospheric molecules is estimated at 0.065 μm, while the surface roughness of the partly polished diamond-coated substrates is from 0.28 μm to 0.57 μm. Even if we press down the slider onto the counter surface, the sliding is still noiseless. This means that even if the attack angle of the upper surface is zero, i. e., even if two sliding surfaces are parallel, the upper surface is lifted by gas flow. This fact denies that the lift force is produced due to the wedge effect. The high pressure enough to float the slider will not appear in Couette flow with a few m/s. Therefore, we consider that the spacing between two sliding surfaces will be in the order of 1 μm or less in such a way that the surface roughness is not negligible. The Knudsen number Kn (= λ/L) will be in the order of 0.1 or larger, where L is the characteristic length of the flow. This shows that the gas flow is in nonequilibrium due to

lack of intermolecular collisions and is governed by the Boltzmann equation and not by the Navier-Stokes equations. Therefore, we use the direct simulation Monte Carlo (DSMC) method [3], which is the stochastic solution of the Boltzmann equation. The DSMC method has been applied to high Knudsen number flows in the air-bearing slider problem [4, 5, 6, 7]. In the previous work [8], we performed numerical simulations of micro-/nanoscale gas flow between two sliding surface, and successfully reproduced lift force large enough to suspend the slider used in Nakamori *et al.*'s experiment [1]. We also found that this effect became notable only for micro-/nanoscale gas flow [9]. In the present study, we investigate the effect of configuration of micro-/nanoscale structure on sliding surface on molecular gas-film lubrication.

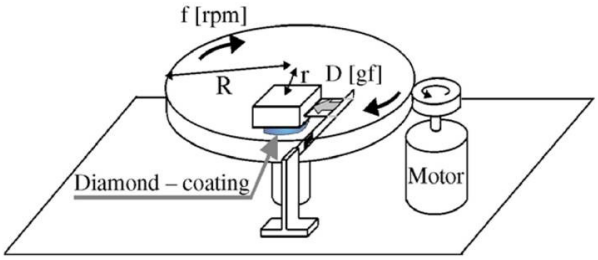

FIGURE 1. Experimental setup of Nakamori *et al*. [1] to measure friction force.

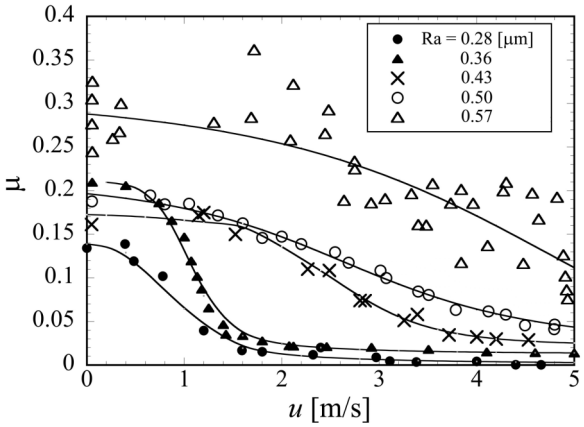

FIGURE 2. Experimental results [1] of the friction force as the function of the relative speed of the surface roughness.

NUMERICAL METHOD

The Scanning Electron Microscope (SEM) image of the partly polished diamond-coated surface is shown in Fig. 3. The image shows that the surface consists of flat parts and concave parts. The flow between two sliding surfaces is three-dimensional. But, for simplicity, we treat the flow as two-dimensional. The computational domain treated here is shown in Fig. 4. The slider surface is above the counter surface. The spacing h between two sliding surfaces is set at 0.14 μm in the present simulation. The counter surface moves rightward with the speed u = 10 m/s. The concave part indicates the surface roughness of the slider. The length l_1, l_4 is the half of width $l_2 + l_3$ of the concave part. The length l_2 is the width of the parallel part of the concave part and the length l_3 is the width of the oblique part of the concave part. We set at $l_1 = l_4 = 11.52$ μm and $l_2 + l_3 = 23.04$ μm in the present simulation. The depth of the concave part is set at $d = 1.44$ μm. The angle θ is the angle of the oblique part to the horizontal line. The periodic boundary conditions are used for both the left and right ends of the domain. Some molecules that run out of the domain through the left or right boundary will come into the domain again through the other boundary, and hence the total number of molecules is unchanged from the initial condition. The flow field is treated as two-dimensional, but molecular motions are treated as three-dimensional.

The computational domain is divided into 20,000 cells depending on the length of the computational domain. The domain is divided into 800 equally partitioned parts in the x-direction and divided into 25 equally partitioned parts in the y-direction. The domain is divided in such a way that each length is smaller than the mean free path. The

gas is atmospheric air with room temperature, T_g = 300 K. The wall temperature is also set at the room temperature, T_w = 300 K. The hard sphere model is used for collision calculation. The diameter of air molecule is set at d = 0.37 nm. Since the mean free time of molecules is 1.4×10^{-10} s, the time step of simulation on molecules is set at 1.4×10^{-11} s. The velocities of molecules reflected on solid wall are determined by using the diffuse reflection model with the wall temperature. Intermolecular collisions in the same cell are calculated stochastically by using the maximum collision number method [10].

The slider surface receives impulsive forces from the incident molecules. The pressure on the slider is obtained by integrating impulsive forces. If N_w simulation molecules collide with the small surface element ΔS of the slider surface during the duration T_{smp}, the pressure on the slider surface is given by

$$p = \frac{W}{T_{smp}\Delta S}\sum_{k=1}^{N_w}\left(mc_{y,k} - mc'_{y,k}\right), \tag{1}$$

where W is the number of real molecules which is represented by one simulation molecule, m is the mass of molecule, $c_{y,k}$ is the y component of the velocity of simulation molecule k.

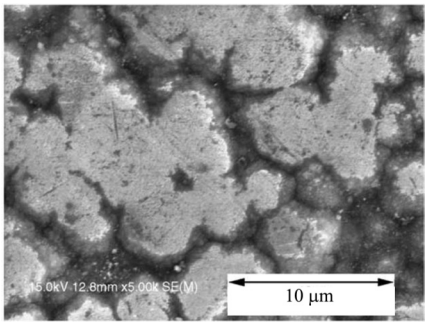

FIGURE 3. Partly polished diamond-coated surface.

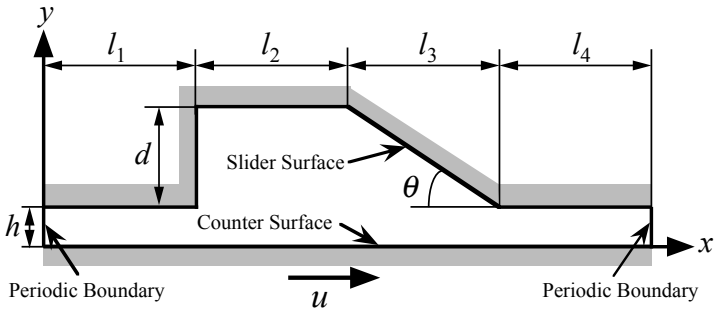

FIGURE 4. Computational domain.

RESULTS AND DISCUSSION

Figure 5 shows the pressure distribution in the case when the shape of right side of the concave part is changed. The upper curve shows the pressure distribution, and the lower diagram shows the shape of the flow channel. The lift force to suspend the slider is given by the difference between the pressure in the figure and the atmospheric pressure p_{atm}. Along the x-axis, the pressure increases in the concave part, and high gas pressure is maintained in the narrow gap. In all cases treated here, the point where the pressure p becomes 1 atm is located at about the center of the concave part. Figure 5 shows that the maximum value of the pressure p increases as the angle θ of the oblique part becomes smaller.

Next, let's consider the mirror-reversed shape for the concave part. Figure 6 shows the pressure distribution in the case when the shape of left side of the concave part is changed. The lower diagram in Fig. 6 shows the shape of

the flow channel. In this case, the length l_2 indicates the width of the oblique part of the concave part and the length l_3 indicates the width of the parallel part of the concave part. As well as Fig. 5, the pressure increases in the concave part along the x-axis and high gas pressure is maintained in the narrow gap. But the shape of pressure distribution in Fig. 6 is quite different from that in Fig. 5. Figure 6 shows that the minimum value of the pressure p decreases as the angle θ of the oblique part becomes smaller.

From the results of Figs. 5 and 6, the pressure p shows the minimum at the inlet of the concave part and shows the maximum at the outlet of the concave part regardless of the configuration of the concave part. Since the spacing h between two surfaces is much less than the depth d of the concave part, if you imagine the cavity flow in the concave part, you can easily understand the reason of low pressure at the inlet and the high pressure at the outlet in the concave part. Figure 7 shows the velocity distribution in the concave part. The velocity distribution indicates vortical flow appears in the concave part. The moving lower surface carries molecules from the left side to the right side. Therefore, the number density at the right edge becomes large and that at the left edge becomes small. Figure 8 shows the distributions of pressure, number density and temperature. Since the temperature is almost uniform, the pressure changes in proportion to the number density. Molecules can be concentrated locally or can be rarefied locally due to low collision frequency in the case of high Knudsen number flows. Therefore, this effect became notable only for micro-/nanoscale gas flow. The strength of the pressure decrease at the inlet of the concave part and the pressure increase at the outlet of the concave part depends on the size of the free space around these points. The angle θ represents the free space around the edge of the concave part. If the space around the inlet is larger, the decrease of number density at the inlet is relaxed by the molecular diffusion from the surrounding. If the space around the outlet is larger, the increase of number density at the outlet is relaxed by the molecular diffusion to the surrounding. Therefore, in Figs. 5 and 6, the intense pressure increase or the intense pressure decrease at the end of the oblique appears in the case when the angle θ is small.

CONCLUSION

We performed the DSMC simulation of the micro-/nanoscale gas flow between the two sliding surfaces. In this study, we investigate the effect of configuration of micro-/nanoscale structure on sliding surface on molecular gas-film lubrication. The pressure increase becomes stronger if the space around the outlet of the concave part is smaller. On the other hand, the pressure decrease becomes stronger if the space around the inlet of the concave part is smaller. Using this knowledge we can propose the desirable shape of the configuration on the slider surface to obtain the strong lift force.

ACKNOWLEDGMENTS

The numerical simulations were carried out using the supercomputer SX-8 at the Institute of Fluid Science of Tohoku University. This work is a collaborative research of the numerical simulation group and the experimental group. Yonemura, who was in charge of the numerical simulation, was supported by Grant-in-Aid for Scientific Research (C) (20560146). Miki, Takeno, and Takagi, who were in charge of the experiment, were supported by Grant-in-Aid for Scientific Research (C) (19560132).

REFERENCES

1. I. Nakamori *et al*., *Diamond Relat. Mater.* **14**, 2122 (2005).
2. T. Abe, T. Takagi, T. M. Sun, T. Uchimoto, and H. Hashimoto, *Diamond Relat. Mater.* **13**, 819 (2004).
3. G. A. Bird, *Molecular Gas Dynamics and the Direct Simulation of Gas Flows,* Clarendon, Oxford (1994).
4. E. S. Oran, C. K. Oh, and B. Z. Cybyk, Annu. Rev. Fluid Mech **30**, 403 (1998).
5. F. J. Alexander, A. L. Garcia, and B. J. Alder, Phys. Fluids **6**, 3854 (1994).
6. W. Huang, D. B. Bogy and A. L. Garcia, Phys. Fluids **9**, 1764 (1997).
7. P. Bahukudumbi, and A. Beskok, J. Micromechanics Microengineering **13**, 873 (2003).
8. S. Yonemura *et all*., *Proceedings of the 26th International Symposium on Rarefied Gas Dynamics, AIP Conference Proceedings,* **1084**, 1153 (2008).
9. S. Yonemura *et al., IFS-Tsinghua University Joint Workshop 2009, 6th International Conference on Flow Dynamics Proceedings*, 584 (2009).
10. K. Nanbu, *IEEE Transactions on Plasma Science* **28**, 971 (2000).

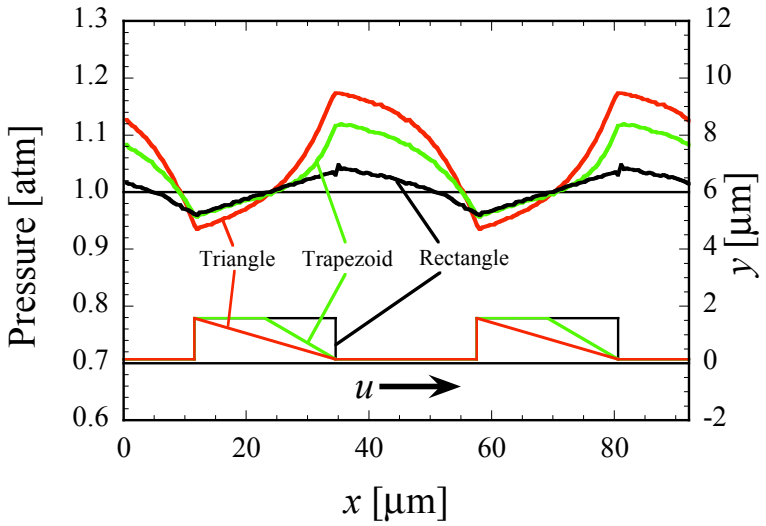

FIGURE 5. The effect of configuration of micro-/nanoscale structure on sliding surface on pressure. (u=10m/s, h=0.14μm, d=1.44μm, l_1= l_4=11.52μm, l_2+ l_3=23.04μm).

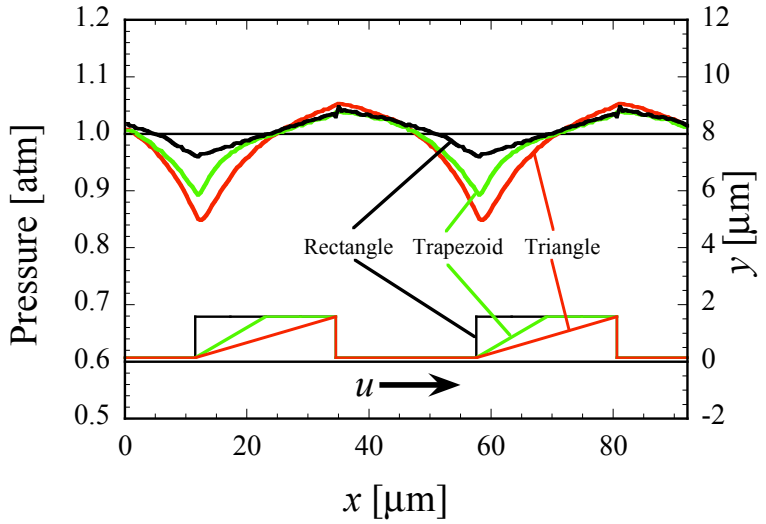

FIGURE 6. The effect of configuration of micro-/nanoscale structure on sliding surface on pressure, where the shape of the concave part is mirror-reversed. (u=10m/s, h=0.14μm, d=1.44μm, l_1= l_4=11.52μm, l_2+ l_3=23.04μm).

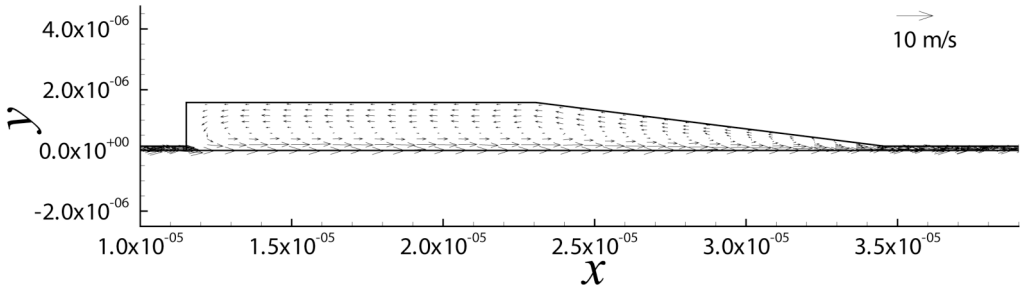

FIGURE 7. Velocity distribution. (u=10m/s, h=0.14μm, d=1.44μm, l_1= l_4=11.52μm, l_2+ l_3=23.04μm).

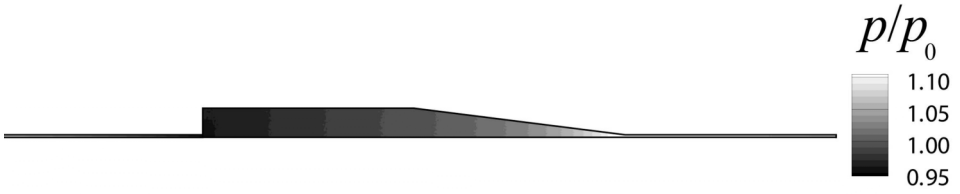

(a) Pressure

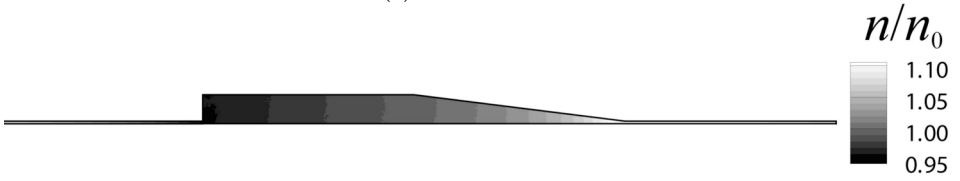

(b) Number density

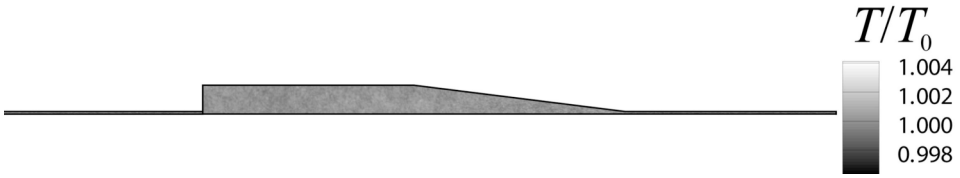

(c) Temperature

FIGURE 8. Distributions of pressure, number density and temperature. (u=10m/s, h=0.14μm, d=1.44μm, l_1= l_4=11.52μm, l_2+ l_3=23.04μm).